PJEST

PJEST

Article

Exploring the Structural and Electronic Properties of Cadmium-doped Zr_3C_2 MXenes for Novel Applications in Advanced Materials and Devices: A DFT study

Bilal Ahmed[1*], Muhammad Bilal Tahir[1,2], Muhammad Sagir[3]

[1]Institute of Physics, Khwaja Fareed University of Engineering and Information Technology, Rahim Yar Khan 64200, Punjab, Pakistan
[2]Centre for Innovative Material Research, Khwaja Fareed University of Engineering and Information Technology, Rahim Yar Khan, Punjab, Pakistan
[3]Institute of Chemical and Environmental Engineering, Khwaja Fareed University of Engineering and Information Technology, Rahim Yar Khan 64200, Punjab, Pakistan.
*Corresponding author e-mail address: raisbilalahmed@gmail.com

ABSTRACT: This research examines the structural and electrical characteristics of Cd-doped Zr_3C_2 MXenes by density functional theory (DFT). Results from structural optimization show that Cd doping changes the lattice properties, which is a sign of local atomic distortions. Calculations of cohesive energy and formation enthalpy show that both pure and Cd-doped structures are thermodynamically stable. Electronic band structure and density of states (DOS) investigations show that adding Cd to Zr_3C_2 adds more electronic states close to the Fermi level while keeping the metallic properties of Zr_3C_2. Partial DOS shows that the d-orbitals of Cd and Zr, as well as the p-orbitals of C, make considerable contributions. These results indicate that the addition of Cd improves the electronic properties of Zr_3C_2 MXenes, positioning them as viable candidates for practical applications in nanoelectronic (e.g., transistors and interconnects), chemical sensors, and energy storage devices, including batteries and supercapacitors.

Keywords: Cadmium (Cd) Doping; Zr_3C_2 MXenes; DFT; Advanced Materials; Energy Storage; Catalysis

Citation: Ahmed, B., Tahir, M. B., & Sagir, M. (2025). Exploring the Structural and Electronic Properties of Cadmium-doped Zr3C2 MXenes for Novel Applications in Advanced Materials and Devices: A DFT study. Pakistan Journal of Emerging Science and Technologies (PJEST), 5(2). https://doi.org/10.58619/pjest.v5i2.181

Academic Editor: Dr. M. Javaid Afzal

Received date: 24-03-2025
Revised date: 19-08-2025
Accepted date: 20-08-2025
Published date: 30-09-2025

1. Introduction

2D materials have attracted great interest in materials research owing to their unusual qualities and likely uses in several sectors including electronics, energy storage, and catalysis [1-3]. Among all these choices, the group of molecules known as MXenes has shown especially great promise [4]. MXenes are compounds produced by removing A elements from MAX phases, in which M is an early transition metal, A is an element from groups 13 to 16, and X is either nitrogen or carbon [5, 6]. MXenes have a broad spectrum of characteristics that one may accurately modify by varying structure and content [7, 8]. The adaptability of MXenes qualifies them for creative applications in advanced materials and systems [9].

Member of the MXene family, the Zr_3C_2 stands out for its remarkable properties including mechanical resilience, great electrical conductivity, and chemical stability [10]. Nevertheless, the introduction of various elements via doping has been proposed and investigated to help Zr3C2 MXenes to develop and increase its capacities [11]. Doping can change surface chemistry, modify band structures, and add new electronic states, therefore customizing the material for particular applications. Within this specific paradigm, doping cadmium (Cd) into Zr_3C_2 provides an interesting route for more study. The special electronic qualities of cadmium might provide Zr_3C_2 with fresh electronic and structural traits, which would be advantageous for its use in sophisticated technologies. The need to find materials with remarkable performance qualities for next uses drives research on Cd-doped Zr_3C_2 MXenes after electrical devices, materials with tailored band gaps, enhanced carrier mobility, and unique surface properties are much sought after [12-15]. Likewise in energy storage devices, materials with superior electrical conductivity, suitable intercalation potential, and structural stability are absolutely vital [16, 17]. MXenes, especially Cd-doped Zr_3C_2, are under much research focus as it is possible to control their properties by doping. Cadmium (Cd) was chosen as a dopant for Zr_3C_2 MXenes because its unique electrical and structural properties make it a good choice for changing the properties of materials. As a post-transition metal with a filled $4d^{10}$ shell and moderate electronegativity, Cd may add more electronic states around the Fermi level without making magnetic instabilities worse. Also, its atomic radius is bigger than Zr's, which is likely to create localized lattice distortions that change the charge distribution and bonding environment. These things can change the density of states a lot and make electronic transit work better. Doping with Cd is a smart way to improve the performance of Zr_3C_2 MXenes in electronic and energy-related uses. Atomic level material analysis now depends critically on DFT [18]. The DFT provides a consistent structure for predicting and understanding the electrical configuration, total energy, and many properties of materials, thereby guiding experimental activities [19]. This work uses DFT to explore, structurally and electrically, Cd-doped Zr_3C_2 MXenes. Finding alterations in the electronic band structure, density of states, and their consequences for device uses takes front stage.

The effects of Cd doping on the structural and electronic characteristics Zr_3C_2 are systematically investigated in this work. DFT computations are applied for the analysis. First, we maximize the atomic structure of both pure and Cd-doped Zr_3C_2 so that we take most stable configurations into account. Further electronic structure simulations clarify the effect of Cd incorporation on the band gap, electronic states close to the Fermi level, and the general

electronic behaviour. By means of a comparison of these properties with undoped Zr_3C_2 and the detection of any developing trends, our aim is to get a better knowledge of the possible applications of Cd-doped Zr_3C_2 MXenes in several sophisticated technologies.

2. Computational Methodology

Cd-doped Zr_3C_2 MXene was computationally analyzed using first-principles calculations inside the framework of density functional theory (DFT). The CASTEP [20] algorithm was used to conduct all simulations, employing a plane wave pseudopotential technique. The exchange-correlation effects were treated using the Generalized Gradient Approximation (GGA) with the Perdew–Burke–Ernzerhof (PBE) functional. A plane-wave cutoff energy of 600 eV was employed to ensure the convergence of total energies and forces. For Brillouin zone integration, a 5 × 5 × 2 Monkhorst-Pack k-point grid was used, which provided a good balance between computational cost and precision in sampling reciprocal space. These parameters were tested for convergence prior to the structural and electronic calculations to ensure the reliability of the results.We optimized the ion positions using the conjugate gradient method. This approach guarantees that the buildings reach their most ideal energy configurations and is quite successful in reducing the general energy of the system. The energy stability was found using a convergence threshold of 1×10^{-5}eV; the Hellmann-Feynman forces on every atom were maintained below 0.02 eV/Å to guarantee structural stability of the system. We used the PBE to give a precise account of the magnetic and electrical characteristics of Cd-doped Zr_3C_2 [21] within the GGA [22]. This functional is highly recognized for providing a consistent balance between computation efficiency and accuracy in electronic structure simulations. Considering the transition metal character of the Zr atoms and the possible complexity generated by Cd doping, the Hubbard U correction was employed to explain the notable correlation effects in the d-orbitals. In our calculations, the Hubbard U parameter used for zirconium (Zr) was 2.00 eV, which corresponds with values reported in literature for like systems.

The structural optimization guaranteed the attainment of the most stable arrangement of Cd-doped Zr_3C_2 by means of a rigorous evaluation of the lattice parameters, bond lengths, and bond angles. Following structural optimization, the electronic characteristics were evaluated by means of electronic band structure computation and DOS. Particularly with relation to the band gap, electronic states close to the Fermi level, and general electronic

properties, the simulations produced useful information concerning the changes induced by Cd doping.

3. **Result and Discussions**

3.1 Structural properties

Thoughtful the stability and possible uses of pure and Cd-doped Zr_3C_2 MXene depends on their structural features. Fig. 1 shows the ideal 2×2×2 super cell comprising pure and doped materials. We thus go over here the structural properties of these materials, including their lattice parameters, symmetry, space group, and atomic locations. The pure Zr_3C_2 MXene structure has hexagonal symmetry distinguished by the space group P63/mmc (No.194). Typical for MXene materials, this symmetry is absolutely essential for their special mechanical and electrical characteristics. Whereas carbon is situated (0.666, 0.333, 0.914), the Zr atoms are found at locations (0, 0, 0) and (0.333, 0.666, 0.843). With a=b=3.51 Å and c=11.22 Å, the lattice factors for the pure Zr_3C_2 are Crucially important for determining the structural framework of the material, these lattice parameters reflect the distances between atoms in the crystal lattice. Four Cd-doped Zr_3C_2 MXene substitutes Cd atoms for four Zr atoms. This substitution influences the lattice properties and general structure: At the designated Zr places inside the hexagonal structure, Cd atoms replace Zr atoms. The lattice parameters c=10.00 Å and a=b=6.14Å define the 4 Cd-doped Zr_3C_2. The expansion of the lattice shown by the increase in the a and b lattice parameters over the pure structure results from Cd's higher atomic radius than Zr. The little drop in the c parameter points to a contraction along the c-axis most likely resulting from changes in bonding and atomic interactions brought about by Cd doping. More noticeable structural changes result when further doping 9 Zr atoms with Cd atoms substituting Zr atoms at the designated Zr sites in the hexagonal configuration. For the 9 Cd-doped Zr_3C_2 MXene, a=b=7.21 Å, c=10.79 Å.

This more notable expansion of the lattice in the hexagonal plane is shown by an increasing in a and b parameters. The little change in the c parameter indicates that the general lattice structure is getting more complicated with increasing Cd concentration, maybe by means of the creation of novel bonding environments and interactions. Understanding how the integration of Cd atoms influences the characteristics of the material depends on these structural changes during Cd doping. Particularly in a and directions, the increase of the lattice parameters shows that Cd doping greatly changes the structural framework of Zr_3C_2 MXenes, hence affecting their mechanical and

electrical characteristics. It is important to realize that, demonstrating their chemical stability, all the MXenes under investigation have optimum energies with negative values. In addition to this, we computed the cohesive energy of these compounds in order to assess the structural stability of these molecules. A compound's cohesive energy is a measurement of the amount of energy that is necessary to shatter the ionic bonds and dissolve the atoms that make up the complex. This energy is quantified as the cohesive energy. This happens when the atoms in the molecule are so far apart from one another that they cannot be possibly connected. Using the following computation, the coherent energy for pure Zr_3C_2 may be determined [23-25] :

$$E_{coh} = \frac{1}{N_{Zr}+N_C}[E_{tot}^{Zr_3C_2} - (N_{Zr}E_{tot}^{Zr_{atom}} + N_C E_{tot}^{C_{atom}})]$$

N_{Zr} and N_C are the symbols that represent the number of Zirconium and carbon atoms that are present in the Zr_3C_2. The Zr_3C_2 tot is a representation of the total energy of materials that are pure Zr_3C_2 MXene samples. The total energies of a single isolated Zr atom and a single isolated C atom are represented by the symbols $E_{tot}^{Zr_{atom}}$ and $E_{tot}^{C_{atom}}$. Through the use following formula, the computation of cohesive energy for doped MXenes was carried out [26-29].

$$E_{coh} = \frac{1}{N_{Zr}+N_{Cd}+N_C}[E_{tot}^{Zr_3-xCd_xC_2} - (N_{Zr}E_{tot}^{Zr_{atom}} + N_{Cd}E_{tot}^{Cd_{atom}} + N_C E_{tot}^{C_{atom}})]$$

$E_{tot}^{Zr_3-xCd_xC_2}$ is the total energy of the Cd-doped Zr_3C_2 MXene unit cell, $E_{tot}^{Zr_{atom}}$, $E_{tot}^{Cd_{atom}}$ and $E_{tot}^{C_{atom}}$are the total energies of isolated Zr, Cd, and C atoms, respectively. N_{Zr}, N_{Cd} and $N_C$represent the number of Zr, Cd, and C atoms in the structure. Table 1 shows the respective computed values of E_{coh} for Zr_3C_2 (pure), Zr_3C_2 (doped 4-atoms) and Zr_3C_2 (doped 8-atoms): − 6.2 eV/atom, − 5.4 eV/atom, and – 5.07 eV/atom, correspondingly. There is no text supplied. In every single one of these instances, the values of cohesive energy that were computed were negative, which indicates that the molecules that were investigated have structural stability. For the purpose of gaining a deeper comprehension of the structural stability, we have performed calculations to determine the formation energy ΔH_f for both the pure and doped compound that are being discussed. The next formula enables one to obtain the enthalpy of formation [30]:

$$\Delta H_f = \frac{1}{N_{Zr}+N_C}[E_{tot}^{Zr_3C_2} - (N_{Zr}E_{grd}^{Zr_{atom}} + N_C E_{grd}^{C_{atom}})]$$

In the Zr_3C_2 unit cell structure, the number of Zirconium and carbon atoms is represented by the symbols N_{Zr} and N_C accordingly. The over-all energy of

the Zr_3C_2 material is described by the expression $E_{tot}^{Zr_3C_2}$. Both $E_{grd}^{Zr_{atom}}$ and $E_{grd}^{C_{atom}}$ are examples of the optimized ground state energies that have been determined for single isolated Zirconium and carbon atoms. The computation of ΔH_f for doped compound were performed with formula [26, 27].

$$\Delta H_f = \frac{1}{N_{Zr}+N_{Cd}+N_C}[E_{tot}^{Zr_3-xCd_xC_2} - (N_{Zr}E_{grd}^{Zr_{atom}} + N_{Cd}E_{grd}^{Cd_{atom}} + N_C E_{grd}^{C_{atom}})]$$

Where N_{Zr}, N_{Cd} and N_C represent the number of zirconium, cadmium, and carbon atoms, respectively. $E_{tot}^{Zr_3-xCd_xC_2}$ denotes the total DFT-calculated energy of the doped MXene supercell and $E_{grd}^{Zr_{atom}}$ $E_{grd}^{Cd_{atom}}$ and $E_{grd}^{C_{atom}}$ refer to the optimized ground-state energies of the isolated Zr, Cd, and C atoms, respectively. The values of ΔHf that were computed are presented in Table 1; for Zr_3C_2 (pure), Zr_3C_2 (doped 4-atoms) and Zr_3C_2 (doped 8-atoms) as – 1.47 eV/mol, – 1.82 eV/mol, and -2.08 eV/mol , respectively.

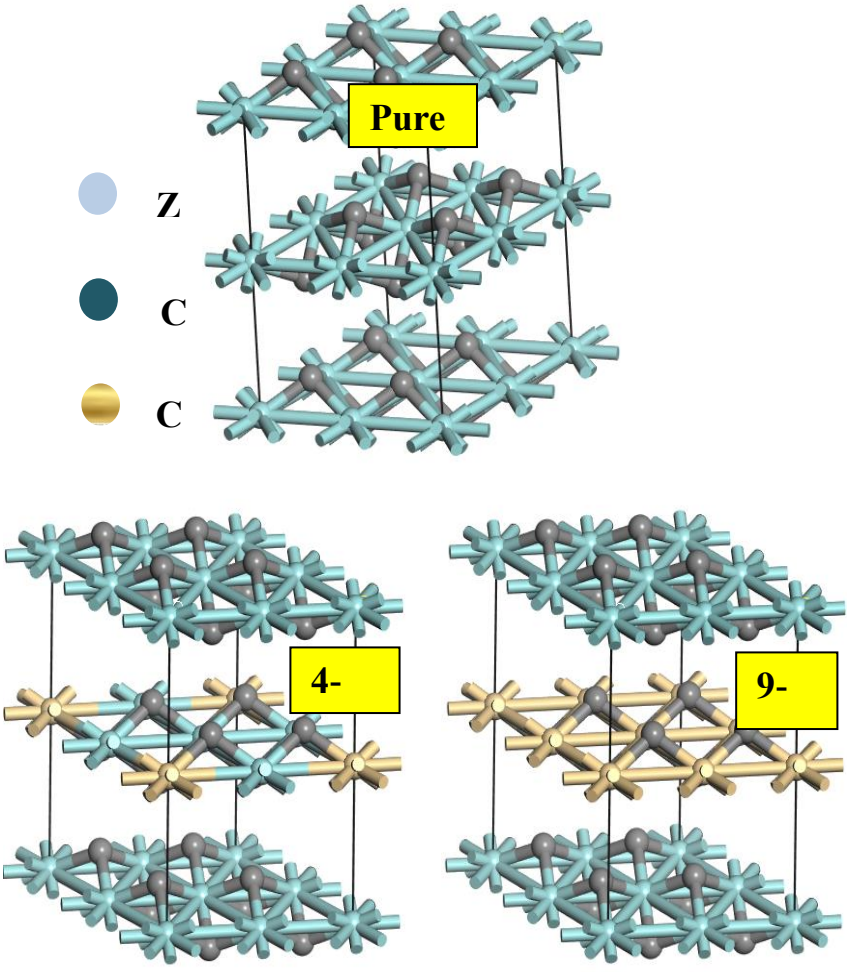

Fig.1: Computed super cell (2×2×2) of Zr_3C_2 compounds

Table 1: Optimized Structural properties

Materials	A_o (Å)	V_o $(Å)^3$	E_o (eV)	E_{coh} (eV/atom)	ΔH_f (eV/mol)
Zr_3C_2 (pure) present study	a = b = 3.51 c=11.22	138.23	-7324.94	-6.2	-1.47
Zr_3C_2 (doped 4-atoms) present study	a = b = 6.14 c=10.00	376.99	-6542.69	-5.4	-1.82
Zr_3C_2 (doped 9-atoms) present study	a = b = 7.21 c=10.79	560.91	-6389.23	-5.07	-2.08
Zr_3C_2 **[31]**	a = b = 3.16 c=20.89	180.78	- 8283.86	-	-1.95
Mo_3C_2 **[31]**	a = b = 3.16 c=18.39	159.09	-1948.05	-	-1.58
Ti_3N_2 **[23]**	a = b = 3.07 c=18.73	153.07	-5464.10	-8.4	-4.38
Hf_3N_2 **[23]**	a = b = 3.14 c=19.66	168.14	-5597.86	-9.2	-4.60
Zr_3N_2 **[23]**	a = b = 3.01 c=20.60	187.18	-4460.88	-8.7	-4.28

3.2 Electronic properties

The electronic characteristics of pure Zr_3C_2 MXene make it evident that it is a metal. The electronic band structure demonstrates that the material doesn't have a band gap because there are states that bridge the Fermi level. The Zr_3C_2 has a high electrical conductivity, which makes it a good choice for applications that need to move charges quickly. The DOS studies show that there are important electronic states at the Fermi level that come largely from the d-orbitals of Zr atoms and the p-orbitals of C atoms. The overlapping states at the Fermi level provide further evidence of the metallic nature of pure Zr_3C_2 MXene. A close look at the band structures (Fig. 2) shows that both pure and Cd-doped Zr_3C_2 MXenes still have their metallic properties, as shown by the continuous bands that cross the Fermi level. When Cd is added, the bands' dispersion properties change in important ways. Partial band flattening is also noticeable near the Fermi level in the doped systems, especially in the 9-Cd-doped setup. This flattening indicates a rise in the effective mass of carriers and potential localization of electronic states, which could affect carrier mobility. Furthermore, more band crossings emerge close

to the Fermi level because the Cd d-orbitals and the Zr/C orbitals mix together. This means that the material has more metallic character. Even while there is no direct opening or closing of the bandgap, the appearance of pseudo gap-like features—areas of lower band density at the Fermi level suggests that states are being redistributed, which could change how electrons move through the material. These changes become more noticeable as the concentration of Cd rises, which shows how important Cd is in changing the electrical structure of Zr_3C_2 MXenes.

Four Cd atoms dope Zr_3C_2 and clearly changes in the electrical properties are observed. Incorporation of Cd atoms, with different electronic configurations than Zr, results in changes in band structure and density of states (DOS). Although the material keeps its metallic qualities, it gains new energy levels at the Fermi level without band gap. The hybridization between the d-orbitals of Cd and the orbitals of Zr and C explains the existence of these additional states mostly. The enhanced number of states at the Fermi level might increase the conductivity of the material and maybe influence its electrical behaviour depending on the conditions. Extra bands crossing the Fermi level in the band structure of the 4 Cd-doped Zr_3C_2 MXene point to an elevated density of accessible electronic states. The electrical properties show more notable change by raising the doping level and adding nine Cd atoms into the Zr_3C_2 structure. Comparatively to the four Cd-doped counterparts, the band structure shows a much higher density of states inside the band gap region. This pattern implies that the number of electronic states in close proximity to the Fermi level increases concurrently with increasing concentration of Cd. Upon examination of the DOS graph, it is evident that there is a greater concentration of states in the vicinity of the Fermi level. This indicates that the amount of electronic activity is increased due to the presence of Cd doping. In uses connected to catalysis or energy storage, this change might be beneficial as it improves electronic states and consequently helps charge transfer mechanisms. Still, the material keeps its metallic qualities free from band gap widening, therefore keeping a zero band gap.

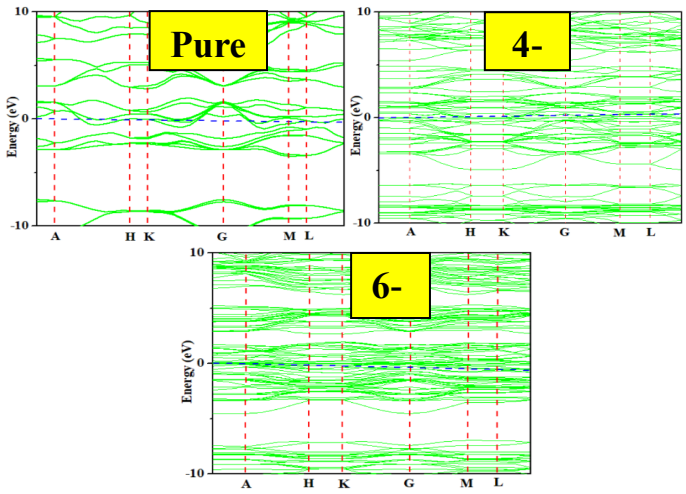

Fig. 2: Band-structure of Zr_3C_2 compounds

A basic metric of great relevance for understanding the electrical properties of materials is the DOS. It indicates the number of electronic states at every energy level that electrons might find to inhabit. We investigate in this work the DOS for both pure Zr_3C_2 MXene and its Cd-doped forms in great detail. We especially pay attention to spotting and talking about the main DOS peaks and their related effects. Two clear peaks show in the DOS for pure Zr_3C_2. The lowest energy range of the valence band suggests the presence of core states mostly derived from the bonding of Zr and C atoms, thereby proposing the peak at -25.93 eV. These states mostly limit a given area and have little effect on the conductivity of the material in general. When the peak at 4.49 eV occurs in the conduction band, it signifies the empty states that are possible locations for electrons to be identified. The position of this peak captures the energy level at which several empty states become reachable.

Four Cd atoms introduced as dopants to Zr_3C_2 causes notable changes in the density of states (DOS), including new peak emergence and changes in current ones. The peak at -26.15 eV is somewhat pushed towards lower energy, implying that the presence of Cd doping influences the core states in line with the unadulterated form. Comparatively to pure Zr_3C_2, the second peak at 4.23 eV likewise occurs in the conduction band and moves somewhat towards lower energy. Cd adds more states, therefore increasing the density of states close to this energy level. The enhanced number of peaks in the DOS spectrum suggests the development of extra electronic states arising from hybridizing Cd and Zr/C orbitals. This suggests more electronic complexity and more opportunity for changes in electronic properties. The density of states (DOS) spectrum gets somewhat more complex by rising the doping to

9 Cd atoms. The -26.41 eV peak moves towards lower energy, implying more marked interactions and changes in the electronic structure brought about by the higher Cd concentration. In the valence band, a clear peak at -8.54 eV indicates the presence of additional states brought on by Cd doping. This implies major changes in the electrical configuration, which can influence the properties of the material.

Peaks in the conduction band at 1.53 eV and 7.76 eV point to the existence of other states that electrons can inhabit. This could raise the conductivity and electrical characteristics of the material. The rather high density of states at these energy levels points to a large number of electronic states inside the conduction band those are accessible. The higher DOS (density of states) can improve the electronic properties, therefore making the material more suitable for uses requiring dynamic electronic behaviour and strong conductivity.

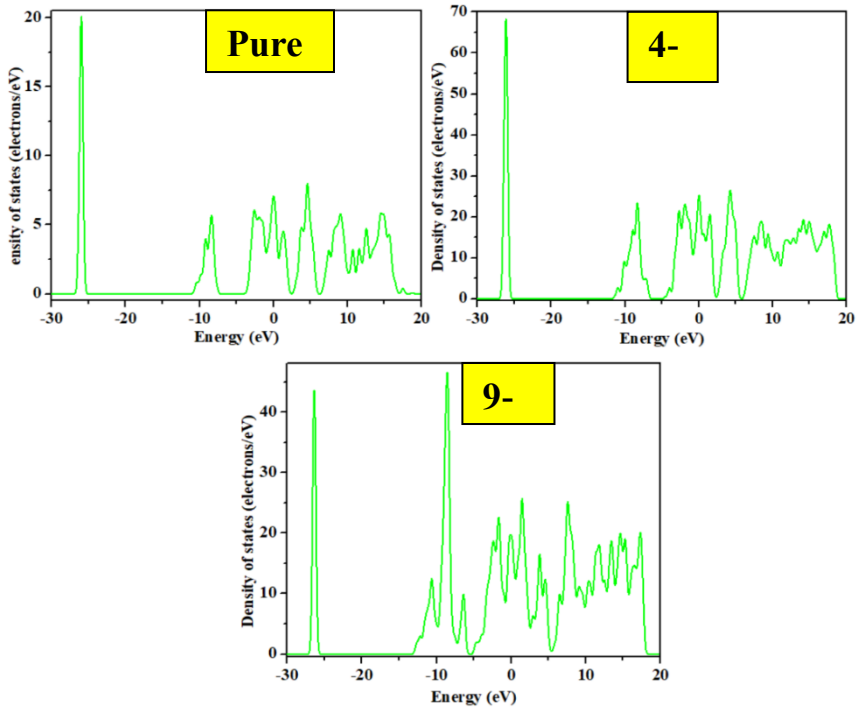

Fig. 3: DOS of Zr_3C_2 compounds

The PDOS provides a more detailed image of the individual contributions of certain atomic orbitals (s, p, and d) in overall electronic assembly of the compound. This picture is more complicated than the one that previous descriptions presented. By use of the PDOS analysis, we may gain a better knowledge of the particular participation of the distinct orbitals in the valence and conduction bands as well as their change in contribution by doping. Characteristics of pure Zr_3C_2 MXene shown by the PDOS study

reveal with a little contribution from p and d orbitals, the valence band is essentially composed of electronic states arising from the Zirconium and carbon atoms. Usually found far in the valence band, these states have little effect on the conductivity of the material. Strong contributions from the Zr d-orbitals and C p-orbitals show in the conduction band. Since they define the states that electrons can inhabit at higher energy levels, these states are very important in defining the electrical properties. Though in less degree than the p and d states, the s-orbitals contribute somewhat to the conduction processes.

Four Cd atoms cause notable changes in the PDOS. Comparatively to the pure Zr_3C_2, the material's valence band shows a somewhat higher fraction of both s and d orbitals presently. This implies that the introduction of Cd doping produces either the displacement of current energy levels or the generation of new ones, hence boosting the interaction of these electron orbitals in the valence band. Greater concentration in the conduction band of both the d-orbitals of Zr and Cd atoms points to an increased number of electron occupancy options. This could raise the electrical conductivity of the component. Furthermore implying a more complex electrical structure is the participation of p and s orbitals in the conduction processes. The partial density of states (PDOS) becomes somewhat more evident by rising the doping to 9 Cd atoms. The rather high concentration of states in the d-orbitals of the valence band points to a significant density peak. These results show that the electronic structure is much influenced by the presence of d-orbitals from Cd and Zr atoms, thereby affecting the valence band mostly. Moreover evident are contributions from both s and p orbitals, implying a larger spectrum of orbital involvement in the valence band. A notable departure from the pure and less substantially doped forms is the great number of states in the conduction band shown by the p-orbitals. This implies that the p-orbitals now significantly influence the conduction band, thereby possibly improving the electrical properties of the material. The conduction processes entail a complex interaction of multiple orbitals including contributions from d and s orbitals.

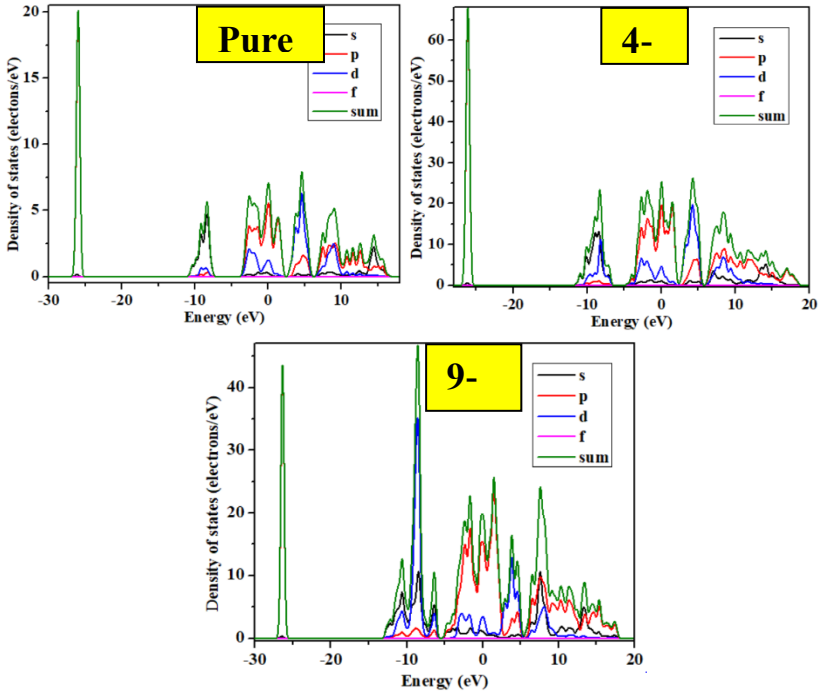

Fig.4: PDOS of Zr_3C_2 compounds

The electronic structure analysis shows that Cd-doped Zr_3C_2 MXenes still have metallic conductivity, but they have a higher density of states around the Fermi level, which suggests that they can move charges better. These materials have these features that make them good candidates for nanoelectronic, such as high-speed transistors, interconnect, and conductive electrodes. The capacity to change the electronic states by adding Cd also makes chemical sensing possible, as the electronic environment can change how sensitive the sensor is to adsorbents. The doped MXenes are also good for electrocatalysis and energy storage devices like supercapacitors and lithium-ion batteries because they are stable and conduct electricity well. Fast electron transport and strong structural integrity are important for these devices. These findings suggest that Cd doping may facilitate the engineering of Zr_3C_2 MXenes for specific functional applications in advanced materials and device designs.

4 Conclusion

Using first-principles DFT simulations, we have shown that adding Cd to Zr_3C_2 MXenes changes their structure and electronic characteristics in a big way. The doping causes the lattice parameters to get bigger while keeping the thermodynamic stability, as seen by the negative cohesive and formation energies. Electronic structure study shows that metallic behavior is still

present and that the density of states at the Fermi level has increased. These changes point to better electronic conductivity. The findings from this study provide a theoretical foundation for subsequent practical investigations and prospective applications of Cd-doped Zr_3C_2 MXenes in nanoelectronic and energy storage technologies.

Author's Contribution: B.A Conceived the idea; Designed the simulated work or acquisition of data; B.A and M.B.T, Executed simulated work, data analysis or analysis and interpretation of data and wrote the basic draft; M.S, Did the language and grammatical edits or Critical revision.

Funding: The publication of this article was funded by no one.

Conflicts of Interest: The authors declare no conflict of interest.

Acknowledgment: The authors would like to thank the advisors who advised for assistance with the collection of data.

References

[1] S. Raza, A. Hayat, T. Bashir, C. Chen, L. Shen, Y. Orooji, *et al.*, "Electrochemistry of 2D-materials for the remediation of environmental pollutants and alternative energy storage/conversion materials and devices, a comprehensive review," *Sustainable Materials and Technologies,* p. e00963, 2024.
https://doi.org/10.1016/j.susmat.2024.e00963
[2] T. Dutta, N. Yadav, Y. Wu, G. J. Cheng, X. Liang, S. Ramakrishna, *et al.*, "Electronic properties of 2D materials and their junctions," *Nano Materials Science,* vol. 6, pp. 1-23, 2024. https://doi.org/10.1016/j.nanoms.2023.05.003
[3] U. Shahzad, M. Saeed, M. F. Rabbee, H. M. Marwani, J. Y. Al-Humaidi, M. Altaf, *et al.*, "Recent progress in two-dimensional metallenes and their potential application as electrocatalyst," *Journal of Energy Chemistry,* 2024. https://doi.org/10.1016/j.jechem.2024.02.068
[4] Y. Jiang, J. Lao, G. Dai, and Z. Ye, "Advanced Insights on MXenes: Categories, Properties, Synthesis, and Applications in Alkali Metal Ion Batteries," *ACS nano,* 2024.
https://doi.org/10.1021/acsnano.3c12543
[5] P. Kumar, R. Rana, A. Kumar, P. Rawat, and J. S. Rhyee, "Structure, Composition, and Functionalization of MXenes," *MXenes: Fundamentals and Applications,* pp. 23-44, 2024. https://doi.org/10.1002/9781119874027.ch2

[6] S. Subramanyam, L. Phor, V. Chaudhary, V. Kaushik, P. Kumar, and S. Chahal, "Progress in MXene synthesis approaches for energy systems: A comprehensive review," *Journal of Energy Storage,* vol. 92, p. 112043, 2024. https://doi.org/10.1016/j.est.2024.112043

[7] B. Jia, Z. Li, T. Zheng, J. Wang, Z.-J. Zhao, L. Zhao, *et al.*, "Highly-sensitive, broad-range, and highly-dynamic MXene pressure sensors with multi-level nano-microstructures for healthcare and soft robots applications," *Chemical Engineering Journal,* vol. 485, p. 149750, 2024. https://doi.org/10.1016/j.cej.2024.149750

[8] N. Xu, F. Wang, P. S. Goh, Y. Liu, X. He, and Y. Wei, "Modification strategies for Ti3C2Tx MXene-based membranes to enhance nanofiltration performance: A review," *Separation and Purification Technology,* p. 127219, 2024.
https://doi.org/10.1016/j.seppur.2024.127219

[9] S. A. Kadam, K. P. Kadam, and N. R. Pradhan, "Advancements in 2D MXene-Based Supercapacitor Electrodes: Synthesis, Mechanisms, Electronic Structure Engineering, Flexible Wearable Energy Storage for Real-World Applications, and Future Prospects," *Journal of Materials Chemistry A,* 2024. https://doi.org/10.1039/D4TA00328D

[10] M. K. Dixit and M. Dubey, "Synthesis of MXenes," *MXenes: Fundamentals and Applications,* pp. 45-64, 2024. https://doi.org/10.1002/9781119874027.ch3

[11] S. A. Thomas and J. Cherusseri, "Recent advances in synthesis and properties of zirconium-based MXenes for application in rechargeable batteries," *Energy Storage,* vol. 5, p. e475, 2023. https://doi.org/10.1002/est2.475

[12] A. Sajjad, M. Faizan, T. A. Alrebdi, G. Murtaza, J. Rehman, X. Shen, *et al.*, "Exploring double perovskites Cs 2 AgSbX 6 (X= Cl, Br, and I) as promising optoelectronic and thermoelectric materials: a first-principles study," *Physical Chemistry Chemical Physics,* vol. 27, pp. 4880-4891, 2025. https://doi.org/10.1039/D4CP04662E

[13] R. Guo, J. Xia, H. Gu, X. Chu, Y. Zhao, X. Meng, *et al.*, "Effective defect passivation with a designer ionic molecule for high-efficiency vapour-deposited inorganic phase-pure CsPbBr 3 perovskite solar cells," *Journal of Materials Chemistry A,* vol. 11, pp. 408-418, 2023. https://doi.org/10.1039/D2TA06092B

[14] D. Strandell, C. Mora Perez, Y. Wu, O. V. Prezhdo, and P. Kambhampati, "Excitonic quantum coherence in light emission from CsPbBr3 metal-halide perovskite nanocrystals," *Nano Letters,* vol. 24, pp. 61-66, 2023.
https://doi.org/10.1021/acs.nanolett.3c03180

[15] Y. She, Z. Hou, O. V. Prezhdo, and W. Li, "Identifying and passivating killer defects in Pb-free double Cs2AgBiBr6 perovskite," *The Journal of Physical Chemistry Letters,* vol. 12, pp. 10581-10588, 2021. https://doi.org/10.1021/acs.jpclett.1c03134

[16] M. M. Baig, I. H. Gul, S. M. Baig, and F. Shahzad, "2D MXenes: synthesis, properties, and electrochemical energy storage for supercapacitors–a review," *Journal of Electroanalytical Chemistry,* vol. 904, p. 115920, 2022.
https://doi.org/10.1016/j.jelechem.2021.115920

[17] N. M. Abbasi, Y. Xiao, L. Zhang, L. Peng, Y. Duo, L. Wang, *et al.*, "Heterostructures of titanium-based MXenes in energy conversion and storage devices," *Journal of Materials Chemistry C,* vol. 9, pp. 8395-8465, 2021. https://doi.org/10.1039/D1TC00327E

[18] B. Ahmed, M. B. Tahir, A. Ali, and M. Sagir, "First-principles screening of structural, electronic, optical and elastic properties of Cu-based hydrides-perovskites XCuH3 (X= Ca and Sr) for hydrogen storage applications," *International Journal of Hydrogen Energy,* vol. 54, pp. 1001-1007, 2024. https://doi.org/10.1016/j.ijhydene.2023.11.239

[19] B. Ahmed, M. B. Tahir, S. Nazir, M. Alzaid, A. Ali, M. Sagir, *et al.*, "An Ab-initio simulation of boron-based hydride perovskites XBH3 (X= Cs and Rb) for advance hydrogen storage system," *Computational and Theoretical Chemistry,* vol. 1225, p. 114173, 2023. https://doi.org/10.1016/j.comptc.2023.114173

[20] B. Ahmed, S. Nazir, A. Khalil, M. B. Tahir, M. Sagir, A. M. Ali, *et al.*, "First-principles study to investigate effect of pressure on electronic and optical properties of KCdCl3 for improved solar cells and optoelectronic applications," *Emergent Materials,* vol. 6, pp. 1697-1705, 2023. https://doi.org/10.1007/s42247-023-00544-6

[21] M. Shafiq, M. B. Tahir, B. Ahmed, A. Dahshan, H. E. Ali, and M. Sagir, "DFT screening of Ga-dopped ScInO3 perovskite for optoelectronic and solar cell applications," *Inorganic Chemistry Communications,* vol. 161, p. 112054, 2024.
https://doi.org/10.1016/j.inoche.2024.112054

[22] B. Ahmed, M. B. Tahir, A. Ali, and M. Sagir, "DFT insights on structural, electronic, optical and mechanical properties of double perovskites X2FeH6 (X= Ca and Sr) for hydrogen-storage applications," *International Journal of Hydrogen Energy,* vol. 50, pp. 316-323, 2024. https://doi.org/10.1016/j.ijhydene.2023.10.237

[23] R. A. Khalil, M. I. Hussain, M. H. Shah, T. I. Al-Muhimeed, G. Nazir, F. Hussain, *et al.*, "The exploration of physical properties of 2D MXenes M3N2 (M= Ti, Hf, Zr, Mo) through the first principles approach:

The energy harvesting materials," *Computational Materials Science,* vol. 238, p. 112947, 2024. https://doi.org/10.1016/j.commatsci.2024.112947

[24] H.-C. Wang, T. Rauch, A. Tellez-Mora, L. Wirtz, A. H. Romero, and M. A. Marques, "Exploring flat-band properties in two-dimensional M 3 QX 7 compounds," *Physical Chemistry Chemical Physics,* vol. 26, pp. 21558-21567, 2024. https://doi.org/10.1039/D4CP01196A

[25] H. Zhang, F. Guégan, J. Wang, and G. Frapper, "Rational design of 2D Janus P 3 m 1 M 2 N 3 (M= Cu, Zr, and Hf) and their surface-functionalized derivatives: ferromagnetic, piezoelectric, and photocatalytic properties," *Physical Chemistry Chemical Physics,* vol. 26, pp. 14675-14683, 2024. https://doi.org/10.1039/D4CP00544A

[26] K. O. Obodo, L. L. Noto, S. J. Mofokeng, C. N. Ouma, M. Braun, and M. S. Dhlamini, "Influence of Tm, Ho and Er dopants on the properties of Yb activated ZnTiO3 perovskite: A density functional theory insight," *Materials Research Express,* vol. 5, p. 106202, 2018. DOI 10.1088/2053-1591/aadaf2

[27] I. C. Onyia, S. O. Ezeonu, D. Bessarabov, and K. O. Obodo, "Density functional theory studies of transition metal doped Ti3N2 MXene monolayer," *Computational Materials Science,* vol. 197, p. 110613, 2021. https://doi.org/10.1016/j.commatsci.2021.110613

[28] A. A. Kistanov, S. V. Ustiuzhanina, M. S. Baranava, D. C. Hvazdouski, S. A. Shcherbinin, and O. V. Prezhdo, "Prediction of Zn2 (V, Nb, Ta) N3 monolayers for optoelectronic applications," *The Journal of Physical Chemistry Letters,* vol. 14, pp. 11134-11141, 2023. https://doi.org/10.1021/acs.jpclett.3c03206

[29] A. A. Kistanov, S. A. Shcherbinin, E. A. Korznikova, and O. V. Prezhdo, "Prediction and characterization of two-dimensional Zn2VN3," *The Journal of Physical Chemistry Letters,* vol. 14, pp. 1148-1155, 2023. https://doi.org/10.1021/acs.jpclett.2c03796

[30] Y. Mao, H. Yang, Y. Sheng, J. Wang, R. Ouyang, C. Ye, *et al.*, "Prediction and classification of formation energies of binary compounds by machine learning: an approach without crystal structure information," *ACS omega,* vol. 6, pp. 14533-14541, 2021. https://doi.org/10.1021/acsomega.1c01517

[31] R. A. Khalil, M. H. Shah, M. I. Hussain, N. H. Alotaibi, S. Mohammad, F. Hussain, *et al.*, "Ab-initio study about the structural, optoelectronic, magnetic, and elastic properties of novel combinations of 2D MXenes M3C2 (M= Zr, Mo) for energy harvesting applications," *Physica B: Condensed Matter,* vol. 685, p. 416016, 2024.

https://doi.org/10.1016/j.physb.2024.416016